TLR2 signaling in skin non-hematopoietic cells induces early neutrophil recruitment in response to *Leishmania major* infection

Catherine Ronet[1,2,*], Katiuska Passelli[1,2,*], Mélanie Charmoy[1,2], Leo Scarpellino[1], Elmarie Myburgh[3], Yazmin Hauyon La Torre[1,2], Salvatore Turco [4], Jeremy C. Mottram[3], Nicolas Fasel[1], Sanjiv A. Luther[1], Stephen M. Beverley [5], Pascal Launois[1,2] and Fabienne Tacchini-Cottier [1,2]

[1]Department of Biochemistry and [2] WHO-IRTC, Faculty of Biology and Medicine, University of Lausanne, Chemin des Boveresses 155, 1066 Epalinges, Switzerland.
[3]Centre for Immunology and Infection, Department of Biology, University of York, Heslington, York, United Kingdom
[4] Department of Biochemistry, University of Kentucky College of Medicine, Lexington, Kentucky, United States of America
[5] Molecular Microbiology Department, Washington University School of Medicine, St. Louis, Missouri, United States of America

* These authors contributed equally

Corresponding author: Fabienne Tacchini-Cottier, Department of Biochemistry, University of Lausanne, Chemin des Boveresses 155, 1066 Epalinges, Switzerland. Phone: +41 21 692 5703; Fax: + 41 21 692 5705

Short Title: TLR2 signaling in skin non-hematopoietic cells triggers neutrophil recruitment following infection with *L. major*

Keywords: Skin, innate immunity, neutrophils, *L. major*, keratinocytes, TLR2, cutaneous leishmaniasis, chemokines, lipophosphoglycans (LPG).

ABSTRACT

Neutrophils are rapidly recruited to the mammalian skin in response to infection with the cutaneous *Leishmania* pathogen. The parasites use neutrophils to establish the disease, however, the signals driving early neutrophil recruitment are poorly known. Here, we identified the functional importance of TLR2 signaling in this process. Using bone-marrow chimeras and immunohistology we identified the TLR2-expressing cells involved in this early neutrophil recruitment to be of non-hematopoietic origin. Keratinocytes are damaged and briefly in contact with the parasites during infection. We show that TLR2 triggering by *L. major* is required for their secretion of neutrophil-attracting chemokines. Furthermore, TLR2 triggering by *L. major* phosphoglycans is critical for neutrophil recruitment impacting negatively on disease development, as shown by better control of lesion size and parasite load in *Tlr2*$^{-/-}$ compared to wild type infected mice. Conversely, restoring early neutrophil presence in *Tlr2*$^{-/-}$ mice through injection of wild type neutrophils or CXCL1 at the onset of infection resulted in delayed disease resolution comparable to that observed in wild type mice. Taken together, our data demonstrate a new role for TLR2-expressing non-hematopoietic skin cells in the recruitment of the first wave of neutrophils following *L. major* infection, a process delaying disease control.

INTRODUCTION

The skin is one of the first barrier and line of defense against invading pathogens. Keratinocytes are a major constituent of the epidermis where they are a source of cytokines and growth factors (Pivarcsi et al., 2004). In response to pathogens, keratinocytes play multiple roles in the control of cutaneous diseases, secreting chemokines and cytokines that contribute to the shaping of the local microenvironment and the attraction of neutrophils to the site of infection.

Leishmaniases are vector-borne diseases transmitted by sand flies that cause a spectrum of diseases manifesting as self-healing cutaneous lesions, mucocutaneous lesions or the more severe visceral form that is fatal if not treated. Following the bite of an infected sand fly, both the epidermis and the dermis where the parasite is deposited, are damaged. There is an increasing interest in better understanding the role of keratinocytes during the onset of an immune response following *Leishmania* infection (Descatoire et al., 2017, Ehrchen et al., 2010, Eidsmo et al., 2007, Gasim et al., 1998, Scorza et al., 2017b). Early neutrophil recruitment is rapidly observed following sand fly infection or needle inoculation of a high dose of *L. major* in mice. Neutrophils can either have a protective or a deleterious impact on disease evolution depending on the infecting *Leishmania* species (spp) and the host, reviewed in (Carlsen et al., 2015, Hurrell et al., 2016).

Healthy human skin keratinocytes express Toll-like receptors 2 (TLR2) (Kawai et al., 2002, Kollisch et al., 2005, Lebre et al., 2007, Li et al., 2009), a TLR that recognizes several pathogen-associated molecular patterns including peptidoglycans (PGN) (Schwandner et al., 1999, Yoshimura et al., 1999), glycosylphosphatidylinositol anchors from protozoan parasites (Campos et al., 2001) and *Leishmania* lipophosphoglycan (LPG) (Spath et al., 2000). Whether TLR2 signaling in skin cells contributes to early neutrophil recruitment at the onset of *L. major* infection and the type of cells involved are unknown.

Here, we demonstrate that within hours of infection, *Leishmania* surface glycoconjugates trigger TLR2 signaling in non-hematopoietic cells including keratinocytes, inducing their release of neutrophil chemoattractants. This mechanism contributes to delayed control of disease.

RESULTS

Leishmania major induces CXC chemokine expression in infected skin and primary keratinocytes

KC (CXCL1), MIP-2 (CXCL2) and lipopolysaccharide-induced LIX (CXCL5) chemokines play a major role in neutrophil recruitment. To investigate their induction in the first hours of infection, *L. major* parasites were injected in the ear dermis (i.d.) of C57BL/6 mice and the kinetics of chemokine mRNA levels was analysed in infected skin during the first hours after infection. Infection increased the mRNA levels of all three chemokine transcripts but with distinct kinetics (**Figure 1a**). To assess the contribution of keratinocytes in chemokine secretion, primary keratinocytes were derived from the skin of C57BL/6 neonates and exposed to *L. major.* Significantly higher levels of KC, MIP-2 and LIX were released in response to *L. major* (**Figure 1b**). To investigate if chemokine secretion resulted from parasite internalization, mCherry-*L. major* parasites were generated. The frequency of infection was analysed by flow cytometry 16 hours after incubation with keratinocytes and compared to that observed following infection of macrophages and neutrophils. A clear $mCherry^+$ population was detected among macrophages and neutrophils but only a low frequency of keratinocytes appeared infected (**Figure 1c**). To further analyze infection of keratinocytes, fluorescent parasites were incubated with primary keratinocytes and parasite presence determined by confocal microscopy 16 hours later. No parasites could be detected within the cells but *Leishmania* interacted with keratinocytes through the flagellar tip, the flagellar base or with the posterior pole of the parasite

(**Figure 1d**). These results suggest that surface recognition of *L. major* by keratinocytes triggers the secretion of MIP-2, KC and LIX by keratinocytes.

TLR2 expression is required to recruit neutrophils after *L. major* infection.

TLRs are pathogen receptors at the surface of various body cells, including keratinocytes. Amongst all TLRs expressed, TLR2 showed the highest mRNA expression level in primary keratinocytes of naïve mice (**Figure 2a**). To assess the role of TLR2 and the downstream adapter protein myeloid differentiation factor-88 (MyD88) in *L. major*-induced rapid neutrophil recruitment in the skin, *Tlr*2$^{-/-}$ and *MyD88*$^{-/-}$ mice were infected i.d. with *L. major* and CXC chemokine levels assessed in the ear skin. Absence of TLR2 and MyD88 in infected ears resulted in a markedly reduced induction of KC, MIP-2 and LIX mRNA (**Figure 2b**). Neutrophil accumulation assessed in the infected ear by flow cytometry and histology peaked at 24 hours post-infection. A significantly reduced neutrophil number was observed in the ear skin of *Tlr*2$^{-/-}$mice (**Figure 2c-e**), accounting for the majority of the decrease observed in absence of MyD88 (**Figure 2c**). These data suggest a predominant role for TLR2 signaling in neutrophil recruitment early after infection and a minor role for other TLRs in this process.

***L. major* LPG triggers TLR2 signaling and neutrophil recruitment**

LPG is one of the most commonly expressed surface molecules on the infectious promastigote parasites that also express other phosphoglycan-containing molecules (PGs) (Sacks et al., 2000). To check the importance of LPG on the TLR2-dependent induction of CXC chemokine secretion by keratinocytes, WT or *Tlr*2$^{-/-}$ primary keratinocytes were isolated and exposed to *L. major* or LPG. Both induced KC and MIP-2 secretion in WT keratinocytes, a process markedly decreased in *Tlr*2$^{-/-}$ keratinocytes (**Figure 3a-b**). To demonstrate the role of LPG in TLR2-induced early neutrophil recruitment *in vivo*, WT mice were infected with WT *L. major*, *L.*

major deficient for LPG alone (*lpg1*$^{-/-}$) or with *L. major* deficient for LPG and all PGs (*lpg2*$^{-/-}$). The complemented "add back" (AB) *lpg1*$^{-/-}$ or *lpg2*$^{-/-}$ parasites were used as controls. Injection of *L. major* deficient in *lpg1*$^{-/-}$ significantly reduced neutrophil recruitment, and adding back *lpg1* (*lpg1*AB) restored the capacity to recruit neutrophils in these parasites (**Figure 3c**). Injection of *lpg2*$^{-/-}$ parasites resulted in even stronger inhibition of neutrophil recruitment to the site of infection, with levels that were comparable to those observed following injection of medium. Adding back *lpg2* to the *L. major* mutant (*lpg2*AB) restored neutrophil recruitment upon infection. (**Figure 3d**). Only a very low number of neutrophils were attracted following injection of WT, AB and *lpg1*$^{-/-}$ or *lpg2*$^{-/-}$ *L. major* parasites in *Tlr2*$^{-/-}$ mice (**Figure 3e**). These data show that LPG and other phosphoglycans present at the surface of *L. major* promastigotes trigger TLR2, resulting in local secretion of chemo-attractants that recruit most of the neutrophils observed at the site of infection during the first 24 hours post-infection.

TLR2 triggering of non-hematopoietic skin cells induces early neutrophil recruitment

To further investigate the source of TLR2-dependent neutrophil chemoattractants in the skin, we generated bone marrow (BM) chimeras as depicted in **Figure 4a**. Eight weeks later, the chimeras were infected with *L. major*. Twenty-four hours post-infection, the presence of $CD11b^{+}Ly6G^{+}$ neutrophils was analyzed by flow cytometry (**Figure 4b**). Neutrophil recruitment was similar in the ear of WT and irradiated WT mice that received *Tlr2*$^{-/-}$ or WT BM (**Figure 4c**). In contrast, irradiated *Tlr2*$^{-/-}$ mice that received WT BM showed markedly reduced neutrophil recruitment 24 hours after *L. major* infection (**Figure 4d**). These data demonstrate that TLR2 expression on non-hematopoietic or radio-resistant cells is required for neutrophil recruitment at the site of parasite inoculation. In addition, two weeks post-infection, decreased parasite burden was observed selectively in irradiated *Tlr2*$^{-/-}$ that received WT BM

(**Figure 4 e-f**), further showing a positive correlation between neutrophil number at the onset of infection and subsequent parasite burden.

To visualize the cells producing early KC and MIP-2, WT mice were infected with *L. major* and 4 hours later, ear skin was isolated and subjected to immunofluorescence staining. High levels of KC staining were observed predominantly in the Epcam^{+} keratinocytes of infected WT and *Tlr*2$^{-/-}$ mice (**Figure 5a** and data not shown), but not when the primary antibody was omitted (**Figure S1**). Similar levels of KC protein were found in the epidermis of naive mice (**Figure 5a**) suggesting this chemokine is constitutively expressed and stored in keratinocytes. In contrast, most of the MIP-2 staining was observed in the dermis and not the epidermis. Similar to KC, MIP-2 protein was present in ear skin of both naïve and infected WT mice (**Figure 5b**) suggesting that this chemokine is also constitutively expressed and stored in dermal cells; no staining was observed in absence of the primary antibody (**Figure S1**). Upon *L. major* infection, dot-like MIP-2^{+} staining appeared in WT dermis, often in close proximity to cells harboring large quantities of intracellular MIP-2 (**Figure 5b, c**), suggesting that the dots represent chemokines released by the dermal MIP-2 source. Interestingly, these MIP-2 dots were only observed locally at the site of swelling and inflammation in WT dermis (**Figure 5c**), in close proximity to infiltrating myeloid cells. In *Tlr*2$^{-/-}$ mice, a similar number of MIP-2^{+} cells was present in naive and infected ear skins, however, the infection triggered less dot-like MIP-2^{+} staining, suggesting less release from the major dermal MIP-2 source. This finding correlated with reduced attraction of myeloid cells, composed mainly of neutrophils (**Figure 5d and Figure S1)**. Quantification of MIP-2^{+} cells and released dots indicated a significant increase in MIP-2^{+} released dots specifically in inflamed areas of *L. major* infected ears of WT but not in *Tlr2*$^{-/-}$ infected ears (**Figure 5e**). CD11b$^{+,}$ NIMP-R14^{+} cells and Ly6G^{+} neutrophils (**Figure 5c-d and S1**) showed only little colocalization with cytoplasmic MIP-2 staining, suggesting that MIP-2 is not being expressed at high levels by monocytes and neutrophils. To further define

the MIP-2 expressing cell type and rule out the contribution of potentially radio-resistant macrophages in early neutrophil recruitment, the dermis was stained for mannose receptor (CD206) and F4/80, two additional dermal macrophage markers. No co-localization with MIP-2 was observed ruling out dermal macrophages as major MIP-2 producing cells. Similarly, no co-localization was observed on $CD207^+$ Langerhans cells (**Figure 5f**). Absence of detectable levels of CD45 expression on most MIP-2^+ cells in the skin of naïve and infected mice confirmed their non-hematopoietic origin. MIP-2^+ cells were negative for VE-cadherin staining and not associated with Collagen type IV^+ basement membranes ruling out lymphatic or endothelial endothelium as well (**Figure 5f**). Collectively, these data indicate that in the first hours after infection, *L. major* triggering of TLR2 on non-hematopoietic skin cells, including mostly keratinocytes and dermal stromal cells, leads to KC and MIP-2 release and thereby neutrophil recruitment.

Absence of TLR2 signaling reduces disease development following *L. major* infection

To assess the global impact of TLR2 on the disease, *Tlr2*$^{-/-}$ mice were infected i.d. with *L. major* and lesion development measured. *Tlr2*$^{-/-}$ mice developed a significantly smaller lesion compared to WT mice as represented by lesion score. To bypass the TLR2 signaling required to attract neutrophil, 10 μg of KC was injected i.d. in *Tlr2*$^{-/-}$ mice at the time of infection, a dose that recruited a similar number of neutrophils compared to that observed following *L. major* infection. *Tlr2*$^{-/-}$ mice injected with KC developed a lesion score similar to that observed in WT mice, while injection of KC in WT mice did not change lesion development (**Figure 6a**). Eighty days post-infection *Tlr2*$^{-/-}$ mice infected in the presence of exogenous KC had a parasite load significantly increased compared to that measured in the ear of similarly infected *Tlr2*$^{-/-}$ mice (**Figure 6b**). To further assess if this phenotype was linked to the restored recruitment of neutrophils, *Tlr2*$^{-/-}$ or WT mice were injected with 10^6 inflammatory WT or *Tlr2*$^{-/-}$ neutrophils

at the time of infection. Of note, the injected inflammatory WT and *Tlr2*$^{-/-}$ neutrophils did not differ functionally (**Figure S2**). Lesion development in *Tlr2*$^{-/-}$ mice that received WT or *Tlr2*$^{-/-}$ neutrophils was similar to that observed in *L. major* infected WT mice (**Figure 6c, d),** with a comparable parasite load observed 35 days post-infection that was significantly higher than that observed in *Tlr2*$^{-/-}$ ears (**Figure 6e**), confirming the absence of functional deficiency in *Tlr2*$^{-/-}$ neutrophils. Conversely, injection of WT or *Tlr2*$^{-/-}$ neutrophils in WT mice did not impact lesion size development (**Figure 6c,d**) and parasite load was similar in WT mice transferred with WT or *Tlr2*$^{-/-}$ neutrophils. Unlike *Tlr2*$^{-/-}$ mice, in addition to transferred neutrophils, *L. major* also massively recruit neutrophils in the infected skin of WT mice, altogether providing a protecting parasite shelter resulting in a subsequent higher parasite load observed in transferred WT mice (**Figure 6f**). Altogether these data demonstrate that *L. major* infection induces rapid TLR2 signaling in skin non-hematopoietic cells, triggering chemokine-mediated neutrophil recruitment, a process favoring transient survival of parasites within neutrophils, delaying subsequent development of a protective response.

DISCUSSION

During the first day of infection, *L. major* is using newly recruited neutrophils as a transient shelter, resisting destruction by the otherwise efficient killing machinery of neutrophils (Regli et al., 2017). We show here that KC, MIP-2 and LIX, three major neutrophil-attracting chemokines are induced locally in the skin in the first hours of infection and we show that pre-stored KC and MIP-2 are released within four hours of infection. Upregulation of KC mRNA and CXCL6 were previously shown to be associated with neutrophil recruitment following *L. major* infection (Muller et al., 2001, Uyttenhove et al., 2011). In addition to chemokines, other factors produced by the parasites (van Zandbergen et al., 2002) or contributed by the sand fly during natural infection such as egested bacteria, salivary gland products and a

proteophosphoglycan gel, are likely to also participate in neutrophil recruitment (de Moura et al., 2010, Dey et al., 2018, Giraud et al., 2018). Thus, multiple factors may contribute and synergize to promote neutrophil recruitment at the site of infection. We show here that during the first hours of infection, TLR2 signaling induced by parasite phosphoglycans (especially LPG) expressed at the surface of the parasite is playing a major role in rapid neutrophil migration to the site of parasite inoculation.

Leishmania and their LPGs were reported to be recognized *in vitro* via TLR2 expressed on macrophages, neutrophils, natural killer cells or dendritic cells (Becker et al., 2003 , Charmoy et al., 2007, de Veer et al., 2003, Faria et al., 2014, Huang et al., 2015, Kavoosi et al., 2010, Tolouei et al., 2013). Prostaglandin E2 secretion by macrophages in response to *L. donovani* was also shown to be TLR2-dependent (Bhattacharjee et al., 2016). However, a role for TLR2 signalling in non-hematopoietic cells had not been reported. Here, we show that in response to *L. major,* TLR2 is the most induced TLR expressed in keratinocytes and that secretion of neutrophil chemoattractants by keratinocytes is TLR2-dependent. Furthermore, recognition of purified *L. major* LPG induced the secretion of chemokines by primary keratinocytes in a TLR2-dependent manner. In vivo, recognition by TLR2 of *L. major* LPG and other PGs was shown to be crucial in the early recruitment of neutrophils following infection with *L. major*. In contrast to macrophages and neutrophils, *L. major* was not internalized by keratinocytes, in line with previous reports (Blank et al., 1993, Mbow et al., 2001, Scorza et al., 2017b). However, as shown by confocal microscopy, *L. major* interacted with keratinocytes at locations where LPG and proteoglycans are enriched (Sadlova et al., 2010). This resulted in the secretion of neutrophil attracting chemokines in a TLR2-dependent process. BM chimera and immunofluorescence microscopy revealed the predominant early role of two main *L. major* induced neutrophil attractants, KC and MIP-2 produced by keratinocytes and dermal stromal cells, respectively. KC and MIP-2 chemokines appeared pre-stored in non-hematopoietic cells

of naïve skin in line with former studies (Johansson et al., 2015, Oynebraten et al., 2004) suggesting that in response to TLR2 triggering rapid release of these pre-stored chemokines can occur, in addition to de novo synthesis. In the epidermis, keratinocytes are the main non-hematopoietic cell type that can sense microbes. Within the dermis, various non-hematopoietic cells exist, including endothelial cells as well as fibroblasts and adipocytes (Lai and Gallo, 2008). We showed that TLR2 induces KC release by keratinocytes. Currently, we cannot exclude that radio-resistant Langerhans cells also produce some KC. Very few keratinocytes, and no endothelial cells expressed MIP-2. The exact source of non-hematopoietic cells releasing MIP-2 remains to be determined. Despite the low or lack of chemokine co-localization with $CD45^{+}$ hematopoietic cells, a few dermal macrophages showed co-staining with MIP-2. Collectively these data suggest that chemokine secretion by macrophages and Langerhans cells do not seem to be responsible for the majority of neutrophils recruited.

Neutrophils play important roles not only in the cutaneous forms but also in the experimental visceral form of the disease (Dey et al., 2018, McFarlane et al., 2008, Sacramento et al., 2015, Smelt et al., 2000). Decreased neutrophil recruitment in the liver and spleen of *L. infantum*-infected *Tlr2*$^{-/-}$ mice was recently described (Sacramento et al., 2017) further implying the importance of TLR2 signalling in the inflammatory response to infection with *Leishmania* spp inducing visceral diseases. *Leishmania* exposure to human primary keratinocytes induced cytokine and chemokine production *in vitro*, however, *L. infantum* was a better inducer than *L. major* (Scorza et al., 2017a), suggesting that there may exist differences between the impact of distinct *Leishmania* spp on keratinocytes function, as previously observed for neutrophils (Hurrell et al., 2016).

We show here that *L. major*-infected *Tlr2*$^{-/-}$ mice developed a significantly smaller lesion size and better controlled parasite load than WT mice. These data are in line with a deleterious role

for neutrophils early in infection. The presence of neutrophils in the skin during the first day of infection, through their release of cytokines and other granule factors (Tecchio et al., 2014), most likely contributes to shaping the microenvironment at the site of infection with a significant impact on subsequent lesion development, in line with previous reports (Hurrell et al., 2015, Peters et al., 2008).

In contrast, *Tlr*2$^{-/-}$ mice infected subcutaneously in the footpad with *L. major* were reported to become transiently susceptible to infection (Halliday et al., 2016). The differences observed between the aforementioned and our study, may be explained by the distinct sites used to inoculate the parasites. During the first hours of infection, neutrophils are poorly recruited following subcutaneous (s.c.) infection while they are strongly recruited following dermal parasite inoculation (Ribeiro-Gomes et al., 2014), a site corresponding to parasite delivery by the sand fly. In line with our data, treatment of mice injected s.c in the footpad with TLR2 agonists, increased neutrophil recruitment to the site of infection (Huang et al., 2015), and treatment with anti-TLR2 antibodies suppressed the anti-inflammatory response but not parasite load (Komai-Koma et al., 2014).

Altogether, we demonstrate here a crucial role for TLR2 signalling in skin non-hematopoietic cells in the early recruitment of neutrophils. This impacts the evolution of cutaneous leishmaniasis, revealing a pathogenic role for early TLR2 signalling in the skin, opening avenues to modulate disease onset.

MATERIALS AND METHODS

Mice

C57BL/6 mice were from Harlan (Envigo, Huntington, United Kingdom). *MyD88*$^{-/-}$, *Tlr2*$^{-/-}$ mice backcrossed onto a C57BL/6 background (from Prof. S. Akira, University of Osaka, Japan) were bred and maintained under pathogen free conditions (UNIL, Epalinges, Switzerland). The maintenance and care of mice complied with and the studies were approved by the ethical guidelines of the state of Vaud Ethic Committees.

Parasites

L. major bearing homozygous deletions of *LPG1 (lpg1*$^{-/-}$*or Δlpg1*$^{-}$*) or LPG2 (lpg2*$^{-/-}$or *Δlpg2*$^{-}$) genes, and their respective complemented "add backs" (AB) were generated previously in the LV39 clone 5 background (Spath et al., 2000, Spath et al., 2003). These and *L. major* LV39 (MRHO/SU/59/P) were maintained as previously described (Tacchini-Cottier et al., 2000).

Keratinocytes culture and chemokine production

Newborn mice primary keratinocytes were cultivated and grown as previously described (Missero et al., 1996). Confluent monolayer of keratinocytes were exposed to 10^6/ml parasites in LCM. Chemokines were measured by ELISAs (R&D, Minneapolis, MN). For immunofluorescence, *L. major* was labeled with CMFDA (Molecular Probes, Eugene, US) fixed with 4% paraformaldehyde, permeabilized with 0.1% Triton and counter stained with rhodamin phallodin (Molecular Probes), mounted and analyzed with Axioplan2 fluorescent microscope (Zeiss, Jena, Germany).

Two-step SYBR green RT-PCR

mRNA was purified (Qiagen, Hilden, Germany) and reverse transcribed using SuperScript II RT (Invitrogen Life Technologies, Carlsbad, CA). Quantitative PCR was performed using the primers listed in the **Supplementary Methods**.

***L. major* inoculation, ear explant and neutrophil recovery**

Mice were injected i.d. with 10^6 stationary phase, wild type or mutants *L. major* or $5x10^5$ metacyclic promastigotes in a volume of 10 µl of DMEM. At the end of the experiment, mice were sacrificed and ears prepared as previously described (Charmoy et al., 2010). Stained cells were analyzed in PBS 2% FCS using a FACSCan or FACS Calibur flow cytometer and analyzed with the FloJo software.

Immunofluorescence and flow cytometry

Ears were prepared for immuno-histology as previously described (Fasnacht et al., 2014). Details are provided in the **Supplementary Methods.** Antibodies against Ly6G, CD4, CD19 (Biolegend) and against CD8, CD11b and CD45, AnnexinV from e-Bioscience, San Diego, CA were used for Flow cytometry. *L. major* infected keratinocytes were counterstained with rhodamine phalloidin (Molecular Probes, Eugene, OR) and analyzed with a fluorescent microscope Axioplan2 coupled with an ApoTome system (Zeiss, Jena, Germany). Immunohistology quantification of MIP-2^+ cells and "dots" was performed using the ImageJ software (University of Wisconsin). The area of determined regions was calculated and the number of MIP-2 positive events/area counted and expressed as events/50.000 µm2.

Generation of mCherry-fluorescent parasites

L. major LV39 mCherry parasites were generated by transfecting log-stage promastigotes with linearized mCherry expression plasmid using the AMAXA nucleofection system (Lonza, Basel, CH), and selecting clones with 50µg/ml hygromycin B (Calbiochem Merck, Darmstadt, Germany) as detailed in the **Supplementary Methods**. In selected experiments, *L. major* was labeled with 5µM CMFDA according to the provider's protocol (Molecular Probes, Eugene, OR). ROS formation was measured with the dihydrodamine (DHR) 123 probe (Sigma) or luminol (Carbosynth) as described by the manufacters.

Bone marrow chimera

Recipient mice were irradiated (900 rad) and reconstituted with 1×10^7 donor mouse BM cells. Six weeks later, mice were bled, and the presence of $CD4^+$, $CD8^+$, $CD19^+$cells was determined by flow cytometry. Chimeric mice were inoculated with *L.major* in the ear and 24 hours post-infection the recruitment of neutrophils were analysed by flow cytometry and two weeks post-infection, parasite load determined by limiting dilution analysis (LDA), (Charmoy et al., 2010).

Transfer of neutrophils

Mice were injected i.p. with $5x10^7$ *L. major* and neutrophils collected 4 hours later and purified using MACS-negative selection (Myltenyi Biotec, Gladbach, Gemany). Purity of neutrophils (>96%) was assessed by flow cytometry. 10 µg of KC, a dose resulting in similar neutrophil number recruited in the infected ear 24 hours post-injection than that observed following infection with 10^6 *L. major* (60360 ± 4002 *versus* 65810 ± 8181 neutrophils/ear) was injected i.d +/- *L. major*. In other experiments, $5x10^5$ C57BL/6 or *Tlr*$2^{-/-}$ neutrophils were co-injected in the ear dermis with 10^6 stationary phase *L. major* promastigotes. Development of ear lesion was measured and a score given (Schuster et al., 2014). Parasite presence was quantified using qRT-PCR using *Leishmania* Kmp11gene-specific primers or limiting dilution analysis as previously described (Ives et al., 2011).

Statistical analysis

Results are expressed as the mean ± SD. Statistical differences between groups were analyzed using T test for unpaired data. A value of $p < 0.05$ was considered significant.

CONFLICT OF INTEREST

There is no conflict of interest

ACKNOWLEDGEMENTS

We thank the Flow Cytometry Facility and the Cellular Imaging Facility (CIF) of the University of Lausanne for technical expertise. This work was supported by Swiss National Foundation for Scientific Research (310030_166651/1 to FC, 120325 to PL and 31003A-166161 to SAL) and the Medical Research Council (MR/KO19384 to JCM) and NIH R01 AI031078 grant to SMB.

REFERENCES

Becker I, Salaiza N, Aguirre M, Delgado J, Carrillo-Carrasco N, Kobeh LG, et al. Leishmania lipophosphoglycan (LPG) activates NK cells through toll-like receptor-2. Mol Biochem Parasitol 2003;130(2):65-74.

Bhattacharjee A, Majumder S, Das S, Ghosh S, Biswas S, Majumdar S. Leishmania donovani-Induced Prostaglandin E2 Generation Is Critically Dependent on Host Toll-Like Receptor 2-Cytosolic Phospholipase A2 Signaling. Infect Immun 2016;84(10):2963-73.

Blank C, Fuchs H, Rappersberger K, Rollinghoff M, Moll H. Parasitism of epidermal Langerhans cells in experimental cutaneous leishmaniasis with Leishmania major. J Infect Dis 1993;167(2):418-25.

Campos MA, Almeida IC, Takeuchi O, Akira S, Valente EP, Procopio DO, et al. Activation of Toll-like receptor-2 by glycosylphosphatidylinositol anchors from a protozoan parasite. J Immunol 2001;167(1):416-23.

Carlsen ED, Liang Y, Shelite TR, Walker DH, Melby PC, Soong L. Permissive and protective roles for neutrophils in leishmaniasis. Clin Exp Immunol 2015;182(2):109-18.

Charmoy M, Brunner-Agten S, Aebischer D, Auderset F, Launois P, Milon G, et al. Neutrophil-derived CCL3 is essential for the rapid recruitment of dendritic cells to the site of Leishmania major inoculation in resistant mice. PLoS Pathog 2010;6(2):e1000755.

Charmoy M, Megnekou R, Allenbach C, Zweifel C, Perez C, Monnat K, et al. Leishmania major induces distinct neutrophil phenotypes in mice that are resistant or susceptible to infection. J Leukoc Biol 2007;82(2):288-99.

de Moura TR, Oliveira F, Rodrigues GC, Carneiro MW, Fukutani KF, Novais FO, et al. Immunity to Lutzomyia intermedia saliva modulates the inflammatory environment induced by Leishmania braziliensis. PLoS Negl Trop Dis 2010;4(6):e712.

de Veer MJ, Curtis JM, Baldwin TM, DiDonato JA, Sexton A, McConville MJ, et al. MyD88 is essential for clearance of Leishmania major: possible role for lipophosphoglycan and Toll-like receptor 2 signaling. Eur J Immunol 2003;33(10):2822-31.

Descatoire M, Hurrell BP, Govender M, Passelli K, Martinez-Salazar B, Hurdayal R, et al. IL-4Ralpha Signaling in Keratinocytes and Early IL-4 Production Are Dispensable for Generating a Curative T Helper 1 Response in Leishmania major-Infected C57BL/6 Mice. Front Immunol 2017;8:1265.

Dey R, Joshi AB, Oliveira F, Pereira L, Guimaraes-Costa AB, Serafim TD, et al. Gut Microbes Egested during Bites of Infected Sand Flies Augment Severity of Leishmaniasis via Inflammasome-Derived IL-1beta. Cell Host Microbe 2018;23(1):134-43 e6.

Ehrchen JM, Roebrock K, Foell D, Nippe N, von Stebut E, Weiss JM, et al. Keratinocytes determine Th1 immunity during early experimental leishmaniasis. PLoS Pathog 2010;6(4):e1000871.

Eidsmo L, Fluur C, Rethi B, Eriksson Ygberg S, Ruffin N, De Milito A, et al. FasL and TRAIL induce epidermal apoptosis and skin ulceration upon exposure to Leishmania major. Am J Pathol 2007;170(1):227-39.

Faria MS, Calegari-Silva TC, de Carvalho Vivarini A, Mottram JC, Lopes UG, Lima AP. Role of protein kinase R in the killing of Leishmania major by macrophages in response to neutrophil elastase and TLR4 via TNFalpha and IFNbeta. FASEB J 2014;28(7):3050-63.

Fasnacht N, Huang HY, Koch U, Favre S, Auderset F, Chai Q, et al. Specific fibroblastic niches in secondary lymphoid organs orchestrate distinct Notch-regulated immune responses. J Exp Med 2014;211(11):2265-79.

Gasim S, Elhassan AM, Khalil EA, Ismail A, Kadaru AM, Kharazmi A, et al. High levels of plasma IL-10 and expression of IL-10 by keratinocytes during visceral leishmaniasis predict subsequent development of post-kala-azar dermal leishmaniasis. Clin Exp Immunol 1998;111(1):64-9.

Giraud E, Lestinova T, Derrick T, Martin O, Dillon RJ, Volf P, et al. Leishmania proteophosphoglycans regurgitated from infected sand flies accelerate dermal wound repair and exacerbate leishmaniasis via insulin-like growth factor 1-dependent signalling. PLoS Pathog 2018;14(1):e1006794.

Halliday A, Bates PA, Chance ML, Taylor MJ. Toll-like receptor 2 (TLR2) plays a role in controlling cutaneous leishmaniasis in vivo, but does not require activation by parasite lipophosphoglycan. Parasit Vectors 2016;9(1):532.

Huang L, Hinchman M, Mendez S. Coinjection with TLR2 agonist Pam3CSK4 reduces the pathology of leishmanization in mice. PLoS Negl Trop Dis 2015;9(3):e0003546.

Hurrell BP, Regli IB, Tacchini-Cottier F. Different Leishmania Species Drive Distinct Neutrophil Functions. Trends Parasitol 2016;32(5):392-401.

Hurrell BP, Schuster S, Grun E, Coutaz M, Williams RA, Held W, et al. Rapid Sequestration of Leishmania mexicana by Neutrophils Contributes to the Development of Chronic Lesion. PLoS Pathog 2015;11(5):e1004929.

Ives A, Ronet C, Prevel F, Ruzzante G, Fuertes-Marraco S, Schutz F, et al. Leishmania RNA virus controls the severity of mucocutaneous leishmaniasis. Science 2011;331(6018):775-8.

Johansson S, Talloen W, Tuefferd M, Darling JM, Scholliers A, Fanning G, et al. Plasma levels of growth-related oncogene (CXCL1-3) associated with fibrosis and platelet counts in HCV-infected patients. Aliment Pharmacol Ther 2015;42(9):1111-21.

Kavoosi G, Ardestani SK, Kariminia A, Alimohammadian MH. Leishmania major lipophosphoglycan: discrepancy in Toll-like receptor signaling. Exp Parasitol 2010;124(2):214-8.

Kawai K, Shimura H, Minagawa M, Ito A, Tomiyama K, Ito M. Expression of functional Toll-like receptor 2 on human epidermal keratinocytes. J Dermatol Sci 2002;30(3):185-94.

Kollisch G, Kalali BN, Voelcker V, Wallich R, Behrendt H, Ring J, et al. Various members of the Toll-like receptor family contribute to the innate immune response of human epidermal keratinocytes. Immunology 2005;114(4):531-41.

Komai-Koma M, Li D, Wang E, Vaughan D, Xu D. Anti-Toll-like receptor 2 and 4 antibodies suppress inflammatory response in mice. Immunology 2014;143(3):354-62.
Lai Y, Gallo RL. Toll-like receptors in skin infections and inflammatory diseases. Infect Disord Drug Targets 2008;8(3):144-55.
Lebre MC, van der Aar AM, van Baarsen L, van Capel TM, Schuitemaker JH, Kapsenberg ML, et al. Human keratinocytes express functional Toll-like receptor 3, 4, 5, and 9. J Invest Dermatol 2007;127(2):331-41.
Li M, Moeen Rezakhanlou A, Chavez-Munoz C, Lai A, Ghahary A. Keratinocyte-releasable factors increased the expression of MMP1 and MMP3 in co-cultured fibroblasts under both 2D and 3D culture conditions. Mol Cell Biochem 2009;332(1-2):1-8.
Mbow ML, DeKrey GK, Titus RG. Leishmania major induces differential expression of costimulatory molecules on mouse epidermal cells. Eur J Immunol 2001;31(5):1400-9.
McFarlane E, Perez C, Charmoy M, Allenbach C, Carter KC, Alexander J, et al. Neutrophils contribute to development of a protective immune response during onset of infection with Leishmania donovani. Infect Immun 2008;76(2):532-41.
Missero C, Di Cunto F, Kiyokawa H, Koff A, Dotto GP. The absence of p21Cip1/WAF1 alters keratinocyte growth and differentiation and promotes ras-tumor progression. Genes Dev 1996;10(23):3065-75.
Muller K, van Zandbergen G, Hansen B, Laufs H, Jahnke N, Solbach W, et al. Chemokines, natural killer cells and granulocytes in the early course of Leishmania major infection in mice. Med Microbiol Immunol 2001;190(1-2):73-6.
Oynebraten I, Bakke O, Brandtzaeg P, Johansen FE, Haraldsen G. Rapid chemokine secretion from endothelial cells originates from 2 distinct compartments. Blood 2004;104(2):314-20.
Peters NC, Egen JG, Secundino N, Debrabant A, Kimblin N, Kamhawi S, et al. In vivo imaging reveals an essential role for neutrophils in leishmaniasis transmitted by sand flies. Science 2008;321(5891):970-4.
Pivarcsi A, Kemeny L, Dobozy A. Innate immune functions of the keratinocytes. A review. Acta Microbiol Immunol Hung 2004;51(3):303-10.
Regli IB, Passelli K, Hurrell BP, Tacchini-Cottier F. Survival Mechanisms Used by Some Leishmania Species to Escape Neutrophil Killing. Front Immunol 2017;8:1558.
Ribeiro-Gomes FL, Roma EH, Carneiro MB, Doria NA, Sacks DL, Peters NC. Site-dependent recruitment of inflammatory cells determines the effective dose of Leishmania major. Infect Immun 2014;82(7):2713-27.
Sacks D, Govind M, Rowton E, Späth G, Epstein L, Turco SJ, et al. The role of phosphoglycans in Leishmania-sand fly interactions. Proc Natl Acad Sci U S A 2000;97:406-11.
Sacramento L, Trevelin SC, Nascimento MS, Lima-Junior DS, Costa DL, Almeida RP, et al. Toll-like receptor 9 signaling in dendritic cells regulates neutrophil recruitment to inflammatory foci following Leishmania infantum infection. Infect Immun 2015;83(12):4604-16.
Sacramento LA, da Costa JL, de Lima MH, Sampaio PA, Almeida RP, Cunha FQ, et al. Toll-Like Receptor 2 Is Required for Inflammatory Process Development during Leishmania infantum Infection. Front Microbiol 2017;8:262.
Sadlova J, Price HP, Smith BA, Votypka J, Volf P, Smith DF. The stage-regulated HASPB and SHERP proteins are essential for differentiation of the protozoan parasite Leishmania major in its sand fly vector, Phlebotomus papatasi. Cell Microbiol 2010;12(12):1765-79.

Schuster S, Hartley MA, Tacchini-Cottier F, Ronet C. A scoring method to standardize lesion monitoring following intra-dermal infection of Leishmania parasites in the murine ear. Front Cell Infect Microbiol 2014;4:67.

Schwandner R, Dziarski R, Wesche H, Rothe M, Kirschning CJ. Peptidoglycan- and lipoteichoic acid-induced cell activation is mediated by toll-like receptor 2. J Biol Chem 1999;274(25):17406-9.

Scorza BM, Wacker MA, Messingham K, Kim P, Klingelhutz A, Fairley J, et al. Differential Activation of Human Keratinocytes by Leishmania Species Causing Localized or Disseminated Disease. J Invest Dermatol 2017a;137(10):2149-56.

Scorza BM, Wacker MA, Messingham K, Kim P, Klingelhutz A, Fairley J, et al. Differential Activation of Human Keratinocytes by Leishmania spp. Causing Localized or Disseminated Disease. J Invest Dermatol 2017b.

Smelt SC, Cotterell SE, Engwerda CR, Kaye PM. B cell-deficient mice are highly resistant to Leishmania donovani infection, but develop neutrophil-mediated tissue pathology. J Immunol 2000;164(7):3681-8.

Spath GF, Epstein L, Leader B, Singer SM, Avila HA, Turco SJ, et al. Lipophosphoglycan is a virulence factor distinct from related glycoconjugates in the protozoan parasite Leishmania major. Proc Natl Acad Sci U S A 2000;97(16):9258-63.

Spath GF, Lye LF, Segawa H, Sacks DL, Turco SJ, Beverley SM. Persistence without pathology in phosphoglycan-deficient Leishmania major. Science 2003;301(5637):1241-3.

Tacchini-Cottier F, Zweifel C, Belkaid Y, Mukankundiye C, Vasei M, Launois P, et al. An immunomodulatory function for neutrophils during the induction of a CD4+ Th2 response in BALB/c mice infected with Leishmania major. J Immunol 2000;165(5):2628-36.

Tecchio C, Micheletti A, Cassatella MA. Neutrophil-derived cytokines: facts beyond expression. Front Immunol 2014;5:508.

Tolouei S, Hejazi SH, Ghaedi K, Khamesipour A, Hasheminia SJ. TLR2 and TLR4 in cutaneous leishmaniasis caused by Leishmania major. Scand J Immunol 2013;78(5):478-84.

Uyttenhove C, Marillier RG, Tacchini-Cottier F, Charmoy M, Caspi RR, Damsker JM, et al. Amine-reactive OVA multimers for auto-vaccination against cytokines and other mediators: perspectives illustrated for GCP-2 in L. major infection. J Leukoc Biol 2011;89(6):1001-7.

van Zandbergen G, Hermann N, Laufs H, Solbach W, Laskay T. Leishmania promastigotes release a granulocyte chemotactic factor and induce interleukin-8 release but inhibit gamma interferon-inducible protein 10 production by neutrophil granulocytes. Infect Immun 2002;70(8):4177-84.

Yoshimura A, Lien E, Ingalls RR, Tuomanen E, Dziarski R, Golenbock D. Cutting edge: recognition of Gram-positive bacterial cell wall components by the innate immune system occurs via Toll-like receptor 2. J Immunol 1999;163(1):1-5.

FIGURE LEGENDS

Figure 1. *L. major* parasites stimulate chemokine secretion by keratinocytes but do not infect them.

(a) Chemokine mRNA levels in ears injected with *L. major* or PBS. Results are expressed as fold increase compared to expression detected in uninfected skin. The data are representative of two experiments. **(b)**. Primary keratinocytes were co-cultured with *L. major* promastigotes at a MOI:10 during 24 hours. Chemokine levels were measured in supernatants by ELISA. *** $p<0.001$ between non-exposed and exposed to *L. major* (**c**) mCherry-expressing *L. major* were incubated with macrophages, neutrophils or primary keratinocytes. The frequency of infection was analyzed by flow cytometry. A representative plot is shown and the frequency given in the bar graph. **(d)** CMFDA-stained *L. major* parasites were incubated with macrophages or keratinocytes for 16 hours. *L. major* presence was analyzed by fluorescent microscopy . Representative pictures are shown.

Figure 2. Neutrophil attraction to *L. major* inoculation site is TLR-2 dependent.

(a) Relative TLR mRNA expression was determined in naive primary keratinocytes. **(b)** mRNA levels of the indicated chemokines were assessed at the indicated time point post-infection in infected ears of WT, *Myd88*$^{-/-}$ and *Tlr2*$^{-/-}$ mice. Results are expressed as fold increase relative to expression in uninfected ears. **(c-d)** WT, *Tlr2*$^{-/-}$ and *MyD88*$^{-/-}$ mice were infected i.d. with 10^6 *L. major* promastigotes. **(c)** Flow cytometry gating strategy and (**d**) mean number ± SD of neutrophils recruited measured at the indicated time by flow cytometry ***: $p<0.001$ comparing *L. major*-infected WT to *Tlr2*$^{-/-}$ or *MyD88*$^{-/-}$ mice. n=4 mice/group . **(e)** Representative Haemotoxylin and Eosin staining of histological sections of ears from WT and *Tlr2*$^{-/-}$ mice, 0, 4 and 24 hours post *L. major* infection. The data are representative of three independent experiments.

Figure 3. Triggering of TLR2 by *L. major* lipophosphoglycans induce neutrophil recruitment to the site of infection

(a-b) Primary WT and *Tlr2*$^{-/-}$ keratinocytes were exposed to *L. major* or *L. major*-purified LPG. 24 hours later, cell-free supernatant was collected and tested for KC and MIP-2 content by ELISA. Representative mean values ± SEM of $n \geq 3$, from one of four experiments are shown. **(c)** Kinetics of neutrophils recruitment in the ears of C57BL/6 mice following injection of WT, *lpg1*$^{-1-}$ (*lpg1* knockout) and *lpg1* add-back (AB) *L. major*, and **(d)** *lpg2*$^{-1-}$ (*lpg2* knockout) and *lpg2* AB *L. major*. **(e)** Kinetics of neutrophil recruitment during the first day after infection in *Tlr2*$^{-/-}$ mice with the indicated *L. major* parasites. The data presented are representative of three independent experiments (n = 3 to 5 mice/group per time point) with similar results. * $p < 0.05$, **$p<0.01$

Figure 4. TLR2 signaling in non-hematopoietic cells is involved in early neutrophil recruitment

(a) WT and TLR2 recipient mice were irradiated and reconstituted with bone marrow (BM) from WT or *Tlr2*$^{-/-}$ donor mice as depicted. As a control WT BM was transferred into irradiated WT mice. 8 weeks later, BM reconstituted mice were inoculated i.d. in the ear with 10^6 *L. major*. **(b)** Representative gating strategy and (**c-d**) number of Ly6G$^+$ neutrophils recruited to the site of injection 24 hours post-infection as quantified by flow cytometry analysis. The data are representative of two independent experiments. (**e-f**) Two weeks post-infection the parasite burden in the infected ears of the indicated chimeras was analyzed by limiting dilution analysis. The data are representative of two independent experiments including ≥ 3 mice/ group. * $p < 0.05$ *** $p<0.001$

Figure 5. MIP-2 and KC producing skin cells in the first hours of *L. major* infection

Staining for **(a)** KC and DAPI in naïve and *L. major* infected WT and *Tlr2*$^{-/-}$ mice 4 hours after infection. 'c': cartilage. (**b**) Staining for MIP-2 and DAPI in WT naïve and infected mice. Magnifications of the indicated area are shown below. The arrows points to MIP-2^{+} dots presumably showing released chemokine. **(c)** Noninflammed and inflammed areas of infected WT skins stained for MIP-2 and for NIMP-R14^{high}CD11b^{+} neutrophils. Below is an enlargement of the defined areas. **(d)** Similar staining as in (**c**) performed for naïve and *L. major* infected *Tlr2*$^{-/-}$ mice. (**e**) Quantification of MIP-2^{+} cells (arrow head) and "dots" (small arrow). The number of MIP-2^{+} events/50'000μm^{2} for WT and *Tlr2*$^{-/-}$ ears is shown. *n*=4 ears/group, representative of 2 independent experiments. (**f**) Co-localisation of MIP-2 was assessed for CD206^{+}F4/80^{+} dermal macrophages, CD207/Langerin^{+} Langerhans cells, CD45^{+} hematopoietic cells, VE-cadherin^{+} endothelium and collagen IV^{+} endothelium associated basement membranes. Representative images are shown. Size bar: 100 μm. *** p<0.001, ns: not significant.

Figure 6. TLR2-dependent neutrophil recruitment impacts lesion development and parasite control.

(a) WT and *Tlr2*$^{-/-}$ mice were co-injected or not with KC at the time of *L. major* infection and lesion score development (± SEM) measured (*n*=5 mice/group). **(b)** The parasite load was determined by qRT-PCR 80 days post-infection.* p<0.05. The data are representative of two experiments. **(c)** WT or *Tlr2*$^{-/-}$ inflammatory neutrophils were injected in the ear dermis of WT or *Tlr2*$^{-/-}$ mice together with *L. major*. Lesion development was monitored using a caliper and compared to that of mice not co-injected with neutrophils. Score size ± SEM of lesions is shown. (*n*=5 mice per group) **(d)** 35 days post-infection representative pictures of ear are shown

(**e-f**) and parasite load was evaluated by qRT-PCR. $p<0.05$, ** $p<0.01$, ns: not significant. Results are representative of two experiments.

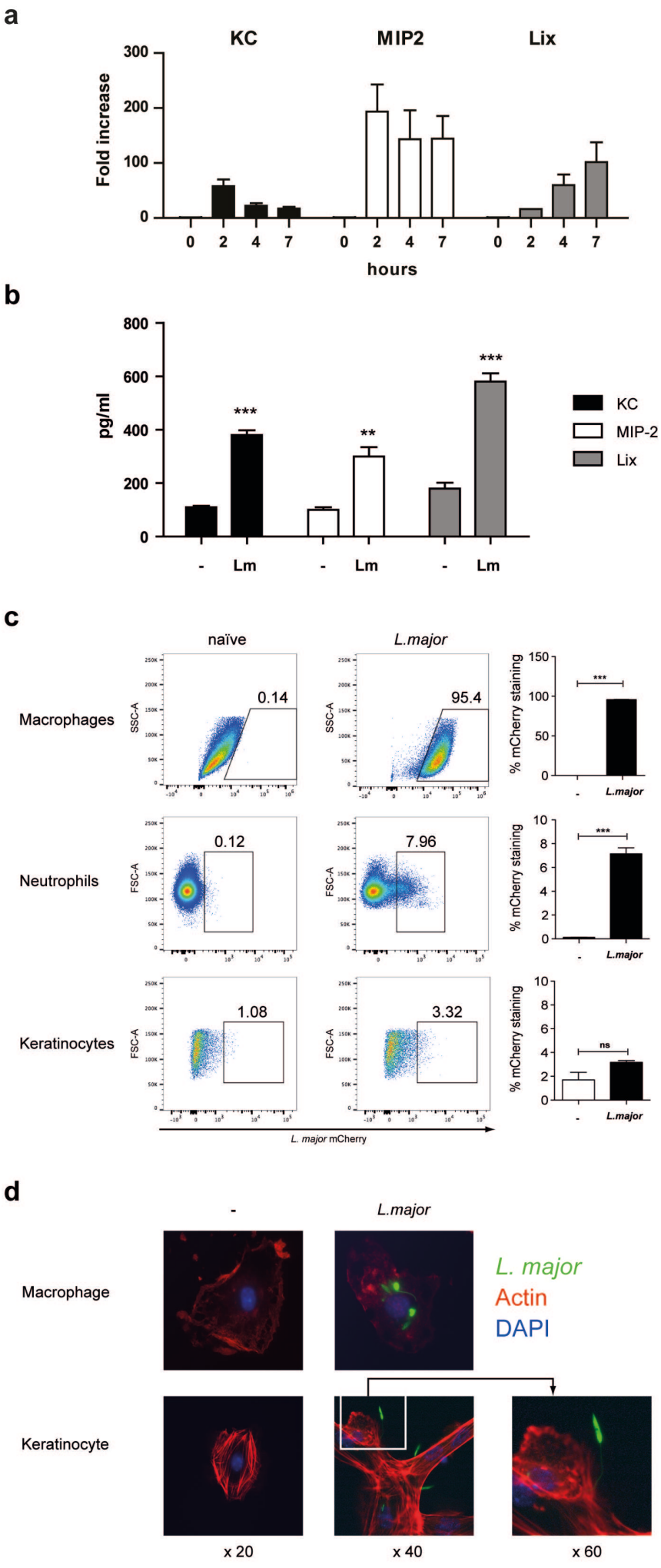
a
KC
MIP2
Lix
Fold increase
300
200
100
0
0 2 4 7 0 2 4 7 0 2 4 7
hours
b
pg/ml
800
600
400
200
0
***
**
***
- Lm - Lm - Lm
KC
MIP-2
Lix
c
naïve
L.major
Macrophages
Neutrophils
Keratinocytes
SSC-A
FSC-A
0.14
95.4
0.12
7.96
1.08
3.32
% mCherry staining
***
ns
- L.major
L. major mCherry
d
-
L.major
Macrophage
Keratinocyte
L. major
Actin
DAPI
x 20
x 40
x 60

Figure 1

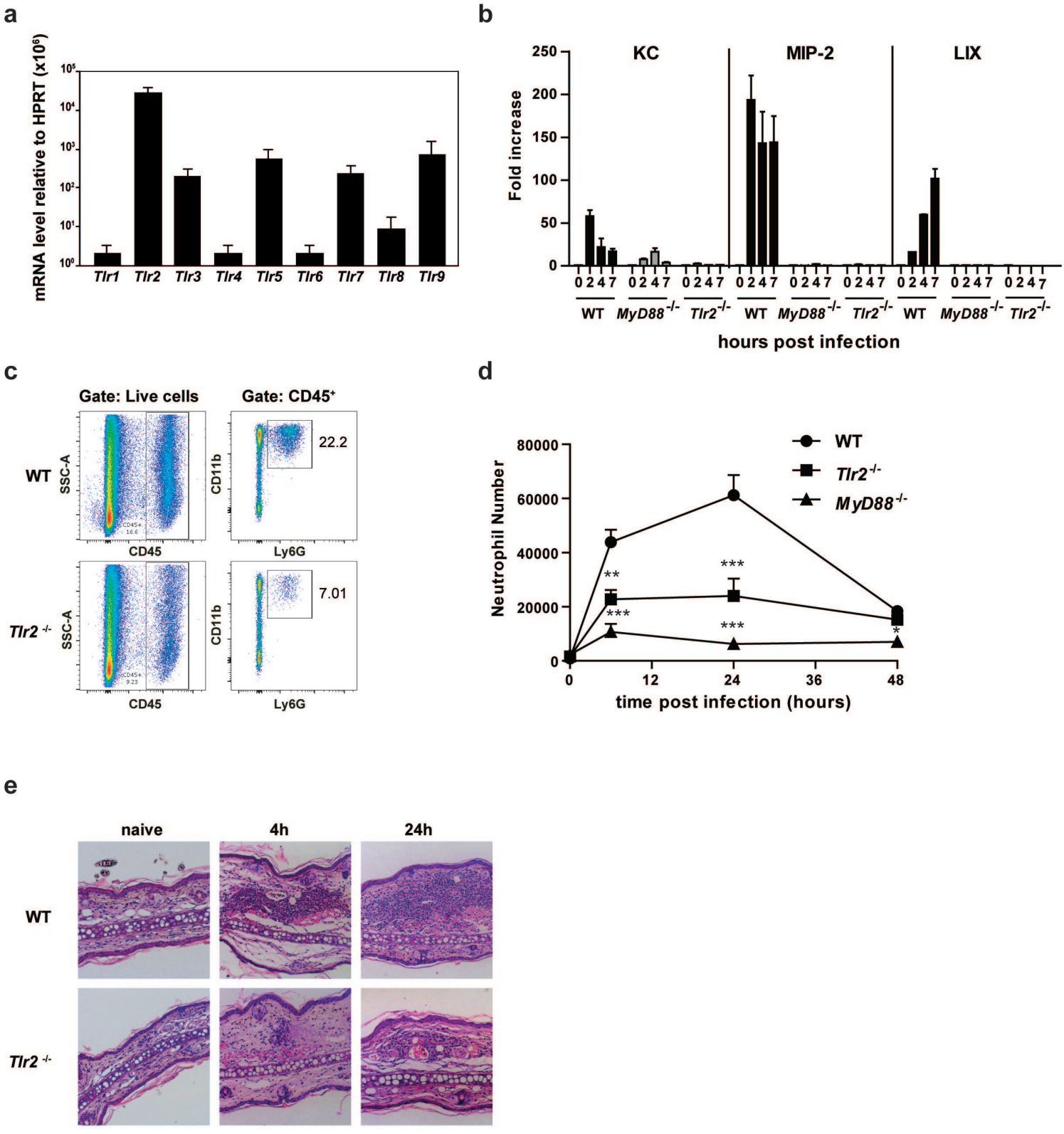
a
mRNA level relative to HPRT (x10^6)
Tlr1 Tlr2 Tlr3 Tlr4 Tlr5 Tlr6 Tlr7 Tlr8 Tlr9
b
KC
MIP-2
LIX
Fold increase
0 2 4 7
WT
MyD88-/-
Tlr2-/-
hours post infection
c
Gate: Live cells
Gate: CD45+
WT
Tlr2 -/-
SSC-A
CD45
CD11b
Ly6G
22.2
7.01
d
Neutrophil Number
WT
Tlr2-/-
MyD88-/-
time post infection (hours)
e
naive
4h
24h
WT
Tlr2 -/-

Figure 2

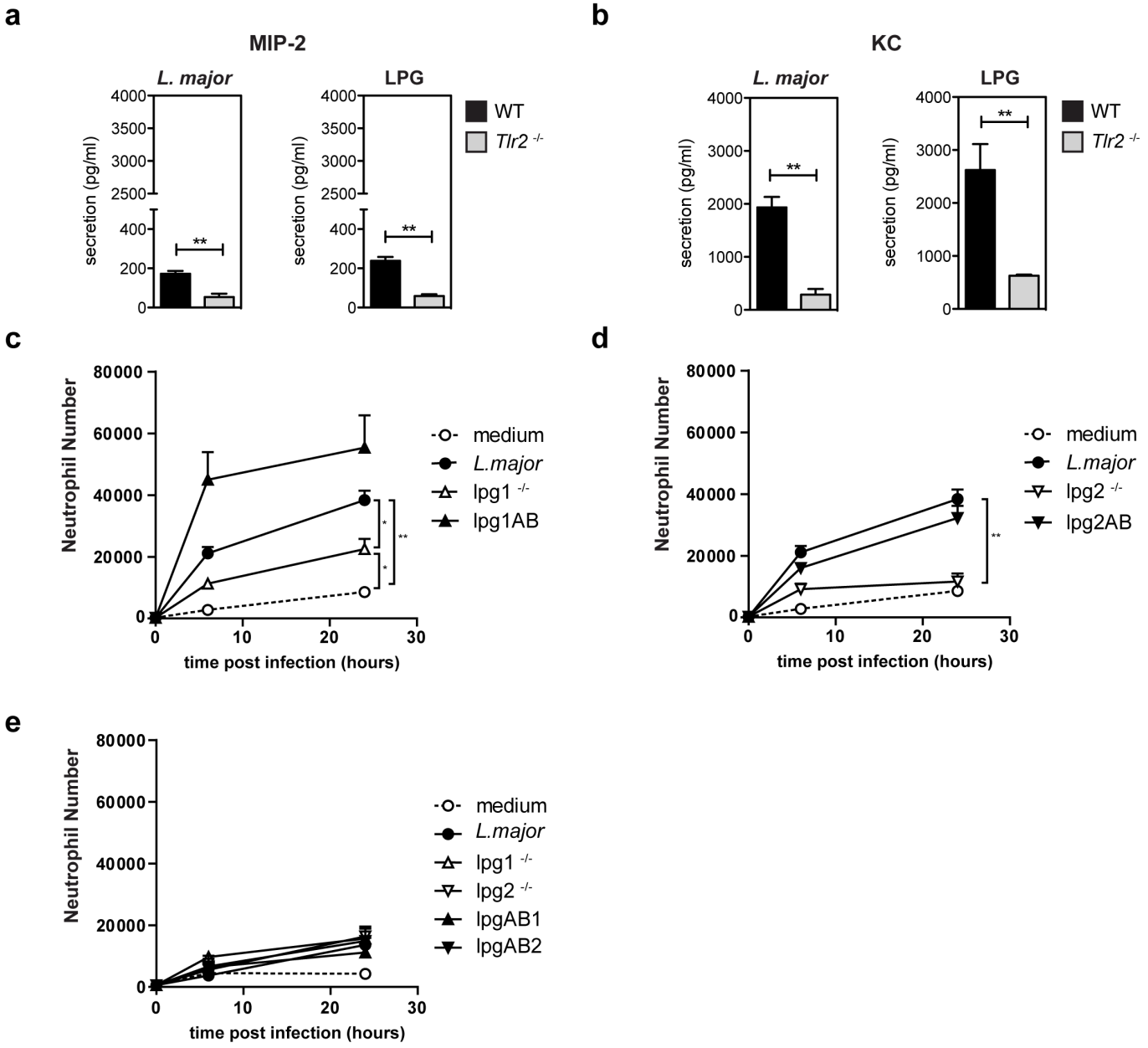
a
MIP-2
L. major
LPG
secretion (pg/ml)
4000
3500
3000
2500
400
200
0
**
WT
Tlr2 -/-
b
KC
L. major
LPG
secretion (pg/ml)
4000
3000
2000
1000
0
**
WT
Tlr2 -/-
c
Neutrophil Number
80000
60000
40000
20000
0
0
10
20
30
time post infection (hours)
medium
L.major
lpg1 -/-
lpg1AB
*
**
*
d
Neutrophil Number
80000
60000
40000
20000
0
0
10
20
30
time post infection (hours)
medium
L.major
lpg2 -/-
lpg2AB
**
e
Neutrophil Number
80000
60000
40000
20000
0
0
10
20
30
time post infection (hours)
medium
L.major
lpg1 -/-
lpg2 -/-
lpgAB1
lpgAB2

Figure 3

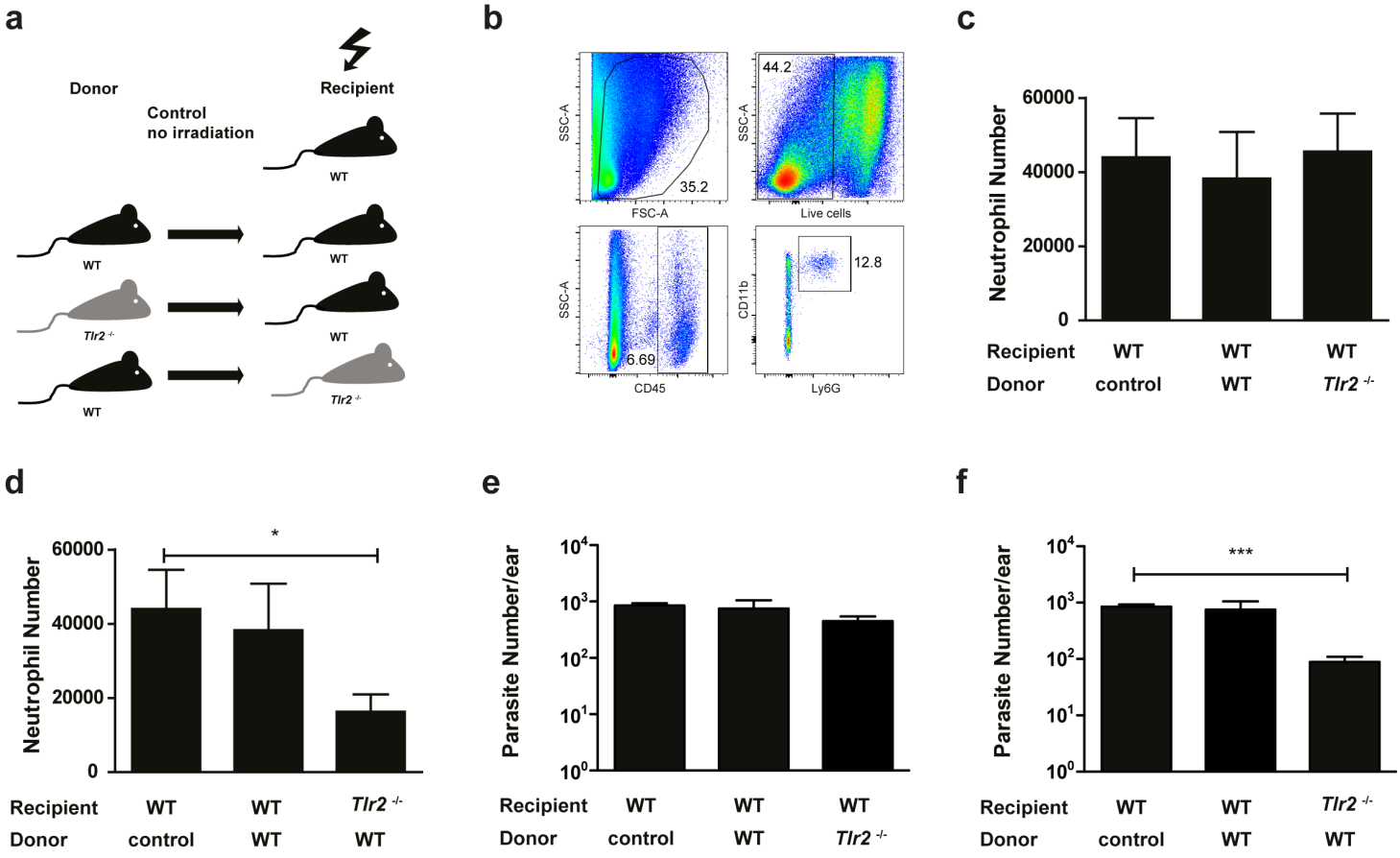
a
Donor
Recipient
Control
no irradiation
WT
WT
WT
WT
Tlr2 -/-
WT
WT
Tlr2 -/-
b
SSC-A
FSC-A
35.2
SSC-A
Live cells
44.2
SSC-A
CD45
6.69
CD11b
Ly6G
12.8
c
Neutrophil Number
60000
40000
20000
0
Recipient WT WT WT
Donor control WT Tlr2 -/-
d
Neutrophil Number
60000
40000
20000
0
*
Recipient WT WT Tlr2 -/-
Donor control WT WT
e
Parasite Number/ear
10^4
10^3
10^2
10^1
10^0
Recipient WT WT WT
Donor control WT Tlr2 -/-
f
Parasite Number/ear
10^4
10^3
10^2
10^1
10^0
***
Recipient WT WT Tlr2 -/-
Donor control WT WT

Figure 4

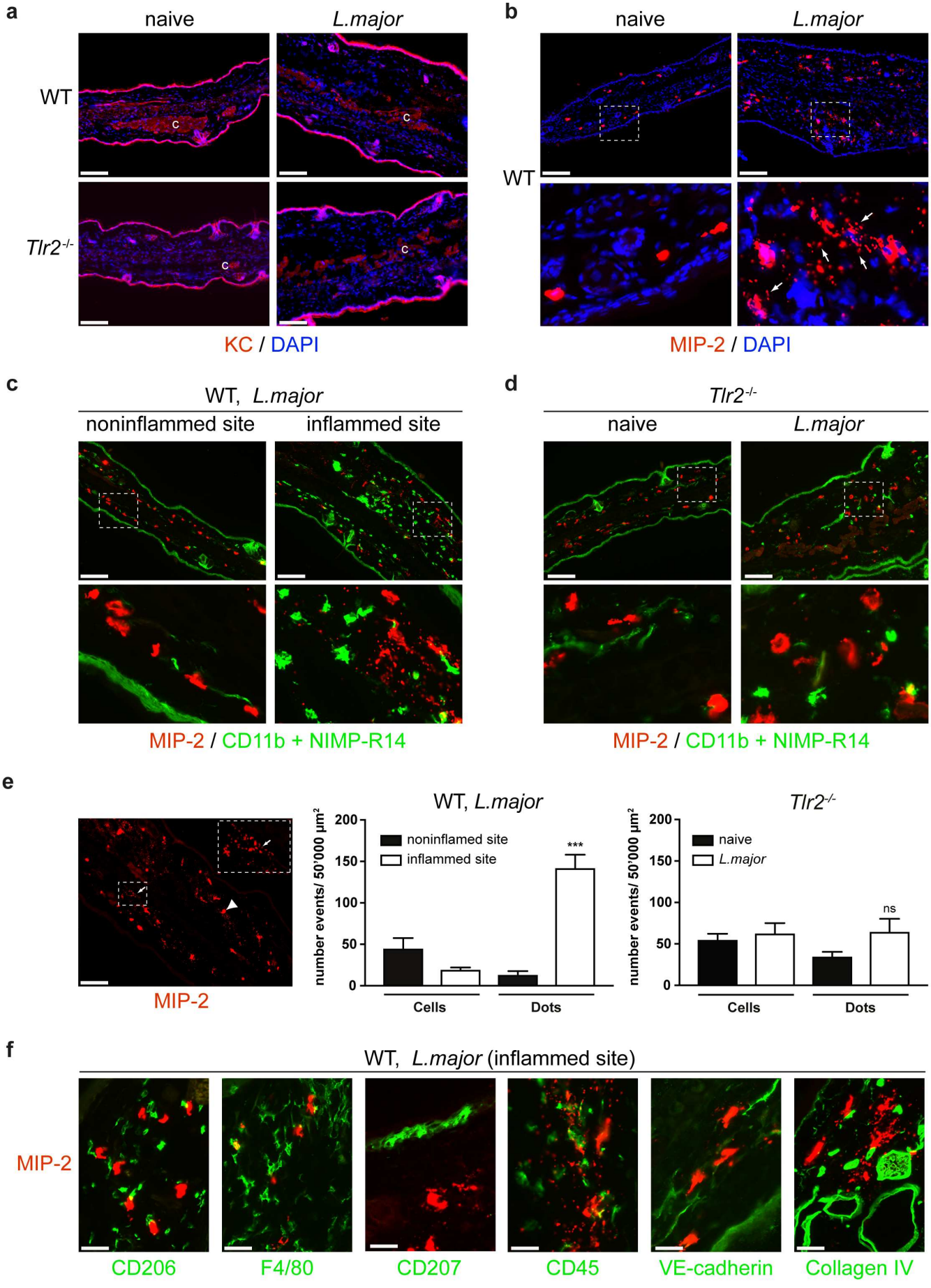
a
naive
L.major
WT
Tlr2-/-
c
KC / DAPI
b
naive
L.major
WT
MIP-2 / DAPI
c
WT, L.major
noninflammed site
inflammed site
MIP-2 / CD11b + NIMP-R14
d
Tlr2-/-
naive
L.major
MIP-2 / CD11b + NIMP-R14
e
MIP-2
WT, L.major
number events/ 50'000 µm²
noninflamed site
inflammed site
***
Cells
Dots
Tlr2-/-
naive
L.major
ns
f
WT, L.major (inflammed site)
MIP-2
CD206
F4/80
CD207
CD45
VE-cadherin
Collagen IV

Figure 5

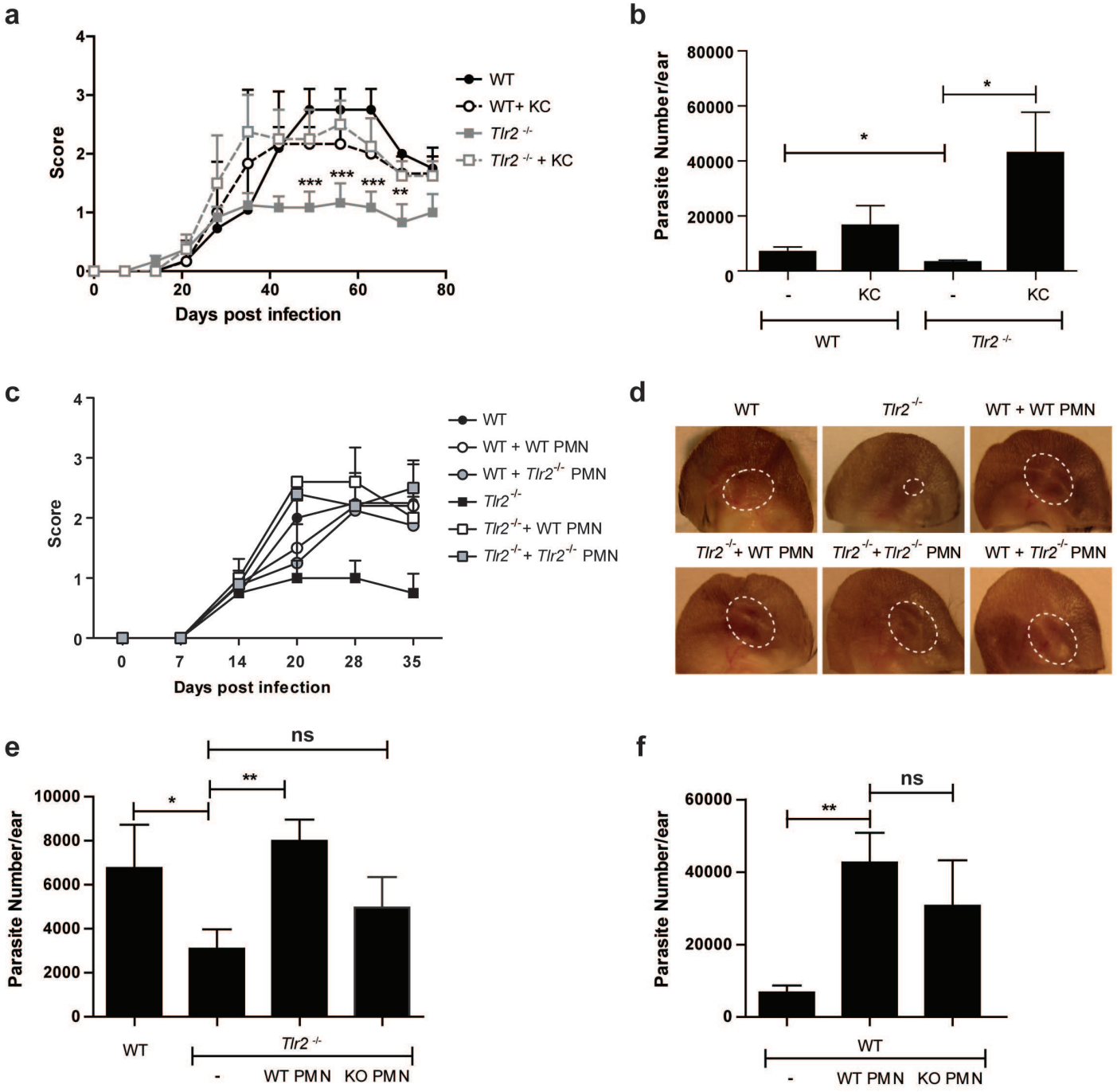
a
Score
Days post infection
WT
WT+ KC
Tlr2 -/-
Tlr2 -/- + KC
***
***
***
**
b
Parasite Number/ear
*
*
-
KC
-
KC
WT
Tlr2 -/-
c
Score
Days post infection
WT
WT + WT PMN
WT + Tlr2-/- PMN
Tlr2-/-
Tlr2-/- + WT PMN
Tlr2-/- + Tlr2-/- PMN
d
WT
Tlr2-/-
WT + WT PMN
Tlr2-/- + WT PMN
Tlr2-/- + Tlr2-/- PMN
WT + Tlr2-/- PMN
e
Parasite Number/ear
ns
**
*
WT
Tlr2 -/-
-
WT PMN
KO PMN
f
Parasite Number/ear
ns
**
WT
-
WT PMN
KO PMN

Figure 6

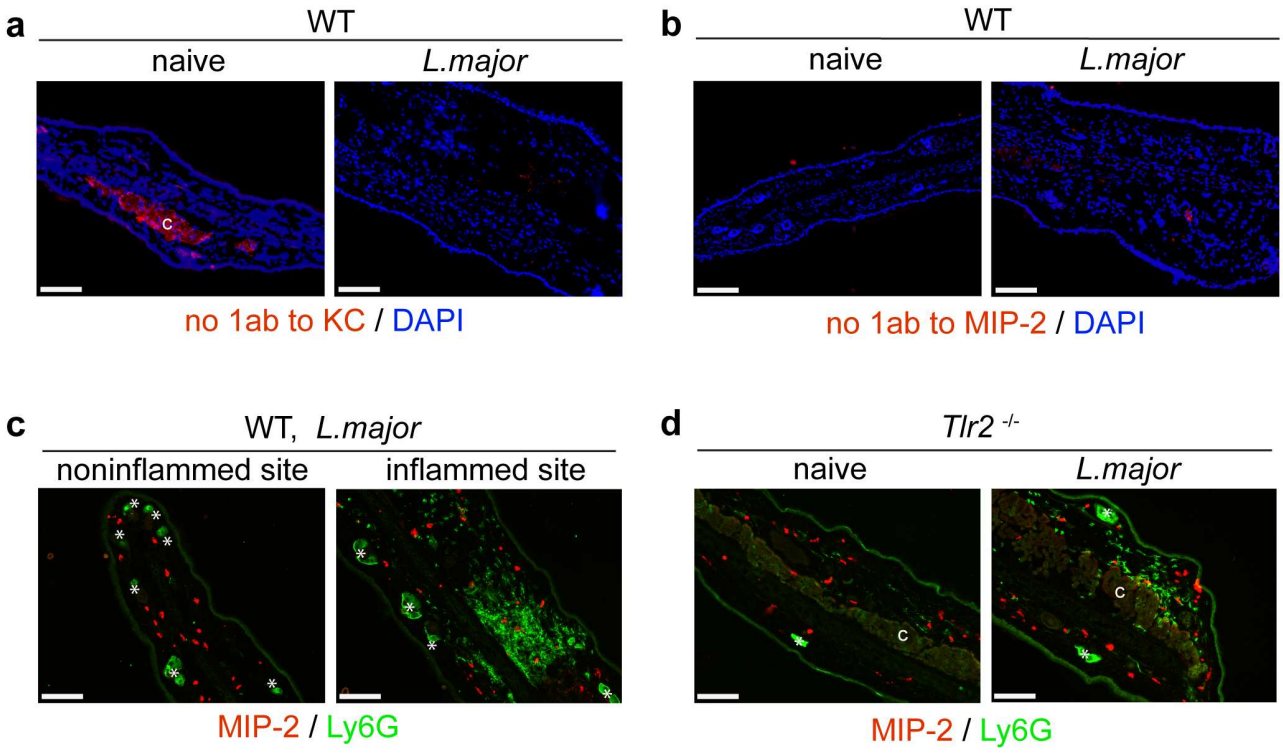

Figure S1. Immunohistology of naïve and *L. major* infected skin. C57BL/6 mice were infected i.d. with $5x10^5$ metacyclic *L. major*. Four hours later ear skin was processed for immunohistochemistry. (**a**) Representative immunofluorescence microscopy images of naïve and *L. major* infected ears stained in absence of the first step KC mAb or (**b**) in absence of the first step mAb against MIP-2. Note non-specific red staining for cartilage. These controls correspond to Figures 5a and 5b respectively. (**c**) Ears were stained with the $Ly6G^+$ neutrophil specific mAb and MIP-2. Staining in infammed and non-inflammed sites is shown. (**d**) Naive and *L. major* infected *Tlr2*$^{-/-}$ ears were similarly processed and stained. Cartilage is shown by a white c. Stars show unspecific staining of hair follicles. These are representative data of 4 ears/ groups.

Supplementary Materials and Methods

Immunofluorescence and flow cytometry

Ears were embedded and frozen in Tissue-Tek O.CT. (Sakura, Benigau, D). Sections of 8μm were prepared as previously described (Fasnacht et al., 2014). Primary antibodies: rabbit polyclonal anti-GRO/KC alpha (Abcam, Cambridge, UK) and anti-MIP-2 (BioRad, Hercules, CA), biotinylated rat anti-CD206 (Biolegend, San Diego, CA), rat antibodies to CD326/EpCAM (G8.8), CD45 (M1/9.4), F4/80 (F4/80), CD11b (M1/70)(all grown in house), NIMP-R14 (Adipogen, Epalinges, CH), Ly6G, CD207 (eBioscience, San Diego, CA) and goat antibodies to collagen IV (Southern Biotech) and VE-cadherin (R&D Systems, Wiesbaden, Germany). The following secondary reagents were used: donkey antibodies to rabbit IgG Cy3, to APC (Jackson ImmunoResearch, Rheinfelden, CH), rat IgG Alexa 488 or to goat IgG Alexa647 or streptavidin Alexa488 (Invitrogen). All slides were stained with DAPI (Sigma-Aldrich, St Louis, MO) and mounted using DABCO solution. Images were acquired on a Zeiss Axiovision microscope with an AxioCam and processed using Adobe Photoshop. Some colors were switched in this process to improve the visualization of signals. For Flow cytometry, mAb against Ly6G, CD4, CD19 are from Biolegend and and mAbs against CD8, CD11b and CD45 and AnnexinV are from e-Bioscience. Keratinocytes infected with *L. major* were fixed with PBS/paraformaldehyde (4%), permeabilized by PBS/Triton (0.1%), counterstained with rhodamine phalloidin (Molecular Probes, Eugene, OR), mounted with Vectashield (Vector Laboratories, Burlingame,CA) and analyzed with a fluorescent microscope Axioplan2 imaging coupled with an ApoTome system (Zeiss, Jena, Germany). Immunohistology quantification of MIP-2$^+$ cells and "dots" was performed using the ImageJ software (University of Wisconsin). Regions of interest were identified, area size calculated and the number of MIP-2 positive events/area counted and expressed as events/50.000 µm2.

Two-step SYBR green RT-PCR

mRNA was purified (Qiagen, Hilden, Germany) and reverse transcribed using SuperScript II RT(Invitrogen Life Technologies, Carlsbad, CA). Quantitative PCR was performed using the following primers listes in the supplementary Methods. KC FW: GCC TAT CGC CAATGAG and RV CTATACTTCGGTTTGGG ; MIP-2 FW ATCCAGAGCTTGAGTGTGACGC and RV AAGGCAAACTTTTTGACGCC ; LIX FW CTA CGGTGGAGTCATAGC and RV CTTGCCGCTCTTCAGTAT. The primers used to amplify TLRs and HPRT were as described (Charmoy et al., 2007).

Generation of mCherry-fluorescent parasites

L. major LV39 mCherry parasites were generated by transfecting log-stage promastigotes with linearized mCherry expression plasmid using the AMAXA nucleofection system (Lonza, Basel, CH), and selecting clones with 50µg/ml hygromycin B (Calbiochem Merck, Darmstadt, Germany). The plasmid (pGL1894) integrates into the ribosomal RNA locus (pSSU-int) (Misslitz et al., 2000) and contains the mCherry gene that is fused at the N-terminus to a mutant version of the first 18 amino acids of *L. major* hydrophilic acylated surface protein B (HASPB G/A) (Prickett et al., 2006) and an E-alpha peptide (Itano et al., 2003). The resulting fusion protein is expressed in the cytosol of *Leishmania* promastigotes and amastigotes (Millington et al., 2010). In selected experiments, *L. major* was labeled with 5µM CMFDA according to the provider's protocol (Molecular Probes, Eugene,

OR). ROS formation was measured with the dihydrodamine (DHR) 123 probe (Sigma) or luminol (Carbosynth) as described by the manufacters.

References:

Charmoy M, Megnekou R, Allenbach C, Zweifel C, Perez C, Monnat K, et al. Leishmania major induces distinct neutrophil phenotypes in mice that are resistant or susceptible to infection. J Leukoc Biol 2007;82(2):288-99.

Fasnacht N, Huang HY, Koch U, Favre S, Auderset F, Chai Q, et al. Specific fibroblastic niches in secondary lymphoid organs orchestrate distinct Notch-regulated immune responses. J Exp Med 2014;211(11):2265-79.

Itano AA, McSorley SJ, Reinhardt RL, Ehst BD, Ingulli E, Rudensky AY, et al. Distinct dendritic cell populations sequentially present antigen to CD4 T cells and stimulate different aspects of cell-mediated immunity. Immunity 2003;19(1):47-57.

Millington OR, Myburgh E, Mottram JC, Alexander J. Imaging of the host/parasite interplay in cutaneous leishmaniasis. Exp Parasitol 2010;126(3):310-7.

Misslitz A, Mottram JC, Overath P, Aebischer T. Targeted integration into a rRNA locus results in uniform and high level expression of transgenes in Leishmania amastigotes. Mol Biochem Parasitol 2000;107(2):251-61.

Prickett S, Gray PM, Colpitts SL, Scott P, Kaye PM, Smith DF. In vivo recognition of ovalbumin expressed by transgenic Leishmania is determined by its subcellular localization. J Immunol 2006;176(8):4826-33.

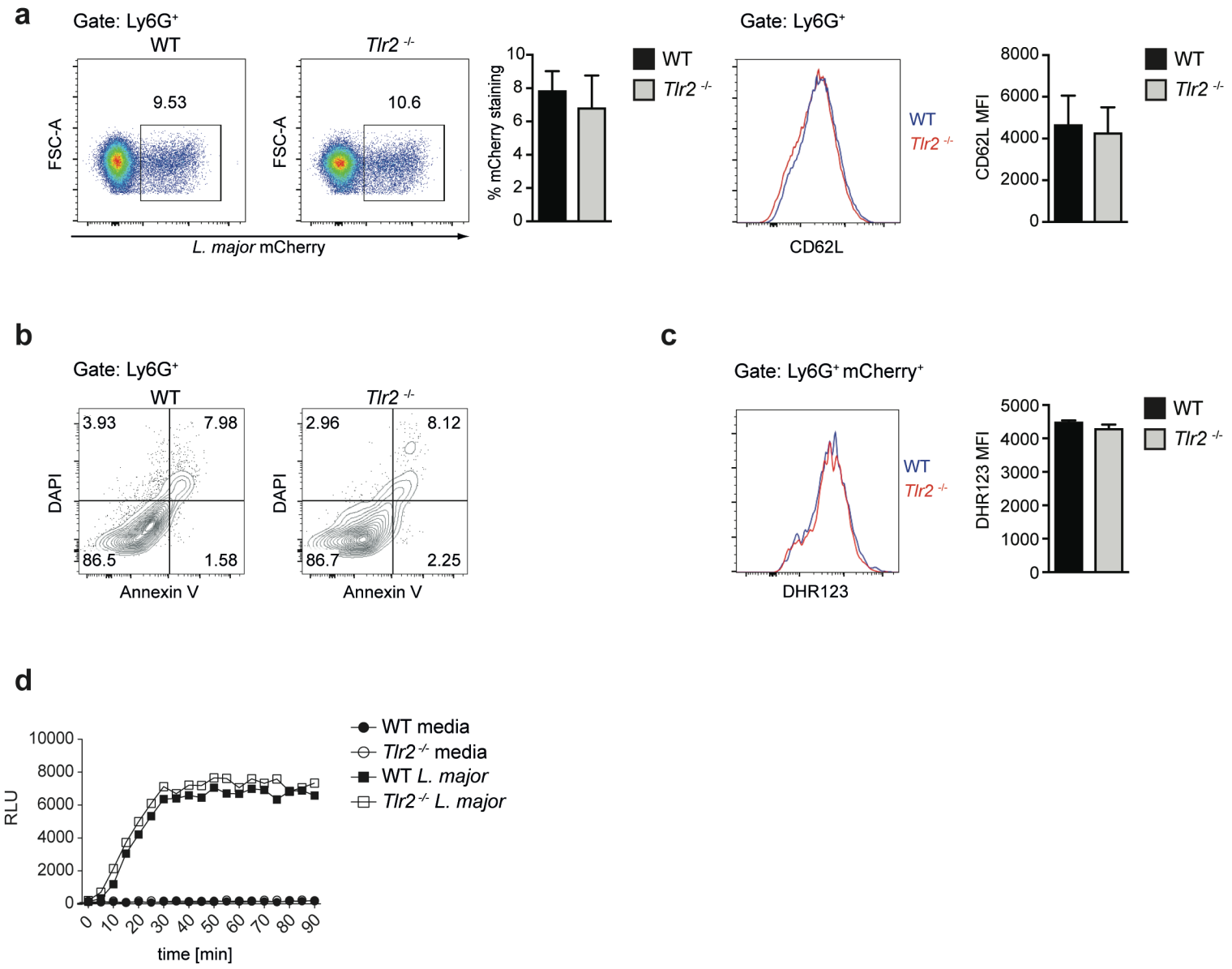

Figure S2. No functional differences are observed between WT and *Tlr2*$^{-/-}$ inflammatory neutrophils. C57BL/6 and *Tlr2*$^{-/-}$ mice were injected i.p. with 10^7 *L. major* and 4 hours later, inflammatory neutrophils were collected and analyzed. (**a**) Representative flow cytometry plot of the frequency of Ly6G$^+$ neutrophils infected with *L. major*-mCherry as analyzed by flow cytometry and represented in the bar graph. Neutrophils activation status was analyzed by CD62L staining. The data are representative of 2 experiments with n=3/ group. (**b**) Inflammatory neutrophils were further analyzed for their apoptotic status, staining with Annexin V and DAPI, revealing early and late apoptosis, respectively (**c**) ROS production was analyzed by flow cytometry using DHR123 These are representative data of two experiments (**d**) C57BL/6 WT and *Tlr2*$^{-/-}$ BM-derived MACS sorted neutrophils were analyzed for ROS production by luminol. These are representative experiments of 2.